$(\sin^2\Theta \cos 2\Omega)$[34,40,41] is expected to be averaged to zero by ligand rotation, must be of opposite sign, but smaller in magnitude than the axial term, whose angular dependence $(3\cos^2\Theta - 1)$[34,40,41] does not average to zero as the ligands rotate. Less pronounced changes in slope were also observed for ortho $CH_3(2)$ and pyrrole H(1), which we have assigned as H_d (Figure 5, dashed lines). All three of these groups are nearest the 5-H of the two 2-MeImH ligands. This region of the complex is relatively less sterically encumbered than is the opposite end, near H_a and ortho $CH_3(1)$ and -(3). The change in slopes of the Curie plots for protons H_d and ortho $CH_3(2)$ and -(4) at -65 °C may indicate the temperature at which rotation ceases as the structure of the molecule is locked into the strongly ruffled form. This form may not only have a different rhombic but also a different axial contribution to the dipolar shift to the three protons whose slopes change at -65 °C than does the freely rotating form, since the value of $3\cos^2\Theta - 1$ will be different for the locked ruffled form than for the average of the forms which are subjected to rotation of the axial ligands.

The EPR spectra of the 2-MeImH complexes of $TMPFe^{III}$ and $(2,6\text{-}Cl_2)_4TPPFe^{III}$ in frozen glasses of CH_2Cl_2 have only one resolved feature, with $g \geq 3.0$.[35] This "large g_{max}" type of EPR signal has previously been shown to occur for bispyridine or hindered imidazole complexes of low-spin Fe(III) porphyrins in which the axial ligands are in perpendicular planes.[16,35,37]

The presence of all possible EXSY cross peaks between chemically equivalent protons (Figure 1B and 2B), together with the absence of cross peaks between free and bound 2-MeImH (as evidenced most clearly in the NOESY map at -29 °C, Figure 1B, in which resonances overlap less than at lower temperatures), indicates that the mechanism of the chemical exchange process is rotation of the bound ligands, as originally suggested by Nakamura and Groves.[13] Such rotation would cause sequential switching of the up/down ruffling distortion of individual *meso*-phenyl groups and indicates that there must be large amplitude motions of the phenyl groups in homogeneous solution, even at relatively low temperatures, if such rotation is to take place. Such fluxionality is seldom detectable, since in the absence of ortho phenyl substituents and/or sterically hindered ligands, preliminary NMR data suggest that axial ligands appear to rotate rapidly, even at -95 °C.[30] In light of the difference in structural model proposed here, the activation parameters measured by Nakamura and Groves[13] for the rotation of the axial 2-MeImH ligands, $\Delta H^{\ddagger} = 12.9$ Kcal/mol, $\Delta S^{\ddagger} = 3.7$ eu,[13] represent the combination of those for ligand rotation and fluxional distortion of the TMP ligand necessary to allow that rotation. Despite the large amplitude motions necessary, these activation barriers are much lower than those due to ligand exchange ($\Delta H^{\ddagger} = 20.1$ Kcal/mol, $\Delta S^{\ddagger} = 40$ eu[42]), and clearly represent those of a totally different chemical exchange process. Further investigations of axial ligand rotation in these "cavity" type porphyrins are currently underway.

Acknowledgment. This research was supported by NIH Grant DK 31038. The Department of Chemistry and Biochemistry at San Francisco State University acknowledges grants from the NIH (RR 02684) and the NSF (DMB-8516065) for purchase of the NMR spectrometers. Bienvenido V. Castillo, III and Sara H. Cody prepared the TMPFeCl. The $(2,6\text{-}Cl_2)_4TPPFeClO_4$ was kindly provided by Professor W. R. Scheidt. The authors thank Drs. D. J. Meyerhoff, J. H. Enemark, and G. N. La Mar for helpful discussions and suggestions.

(41) Horrocks, W. D.; Greenberg, E. S. *Biochim. Biophys. Acta* **1973**, *322*, 38-44. Horrocks, W. D.; Greenberg, E. S. *Mol. Phys.* **1974**, *27*, 993-999.

(42) Satterlee, J. D.; La Mar, G. N.; Bold, T. J. *J. Am. Chem. Soc.* **1977**, *99*, 1088. The entropy of activation has been recalculated from the data provided in that paper.

Charge Transfer across Oblique Bisporphyrins: Two-Center Photoactive Molecules

Anne M. Brun,[†] Anthony Harriman,*[,†] Valérie Heitz,[‡] and Jean-Pierre Sauvage*[,‡]

Contribution from the Institut de Chimie, Université Louis Pasteur, 67000 Strasbourg, France, and Center for Fast Kinetics Research, The University of Texas at Austin, Austin, Texas 78712.
Received June 4, 1991

Abstract: A bisporphyrin, comprising gold(III) and zinc(II) porphyrins held in an oblique orientation via a 1,10-phenanthroline spacer, undergoes intramolecular electron transfer with almost unit quantum efficiency on excitation with visible light. The reaction pathway and kinetics vary according to which porphyrin absorbs the incident photon, but the net reaction involves intramolecular electron transfer from zinc porphyrin (ZnP) to gold porphyrin (AuP^+). Thus, the ZnP excited singlet state transfers an electron to the appended AuP^+. Excitation of the AuP^+ generates the triplet excited state which abstracts an electron from the ZnP (77%) or transfers electronic energy to it (15%). The ZnP triplet state also transfers an electron to the appended AuP^+. Similar processes are observed with the corresponding gold/free-base bisporphyrin.

Photoinduced energy or electron transfer between porphyrins, which is of interest both for understanding natural photosynthesis and for the design of molecular electronic devices, has been demonstrated for various supramolecular systems.[1-7] Singlet energy transfer, occurring by the Förster mechanism, has been described for a range of covalently linked zinc(II)/free-base bisporphyrins possessing different types of spacer group.[5] These studies have been extended to larger arrays in an effort to mimic

[†] University of Texas.
[‡] Université Louis Pasteur.

(1) Harriman, A. In *Energy Resources Through Photochemistry and Catalysis*; Gratzel, M., Ed.; Academic Press: London, 1983; p 163.
(2) Wasielewski, M. R. *Photochem. Photobiol.* **1988**, *47*, 35.
(3) Gust, D.; Moore, T. A. *Science* **1989**, *244*, 35.
(4) Mataga, N. In *Photochemical Energy Conversion*; Norris, J. R., Meisel, D., Eds.; Elsevier: New York, 1989; p 32.

0002-7863/91/1513-8657$02.50/0

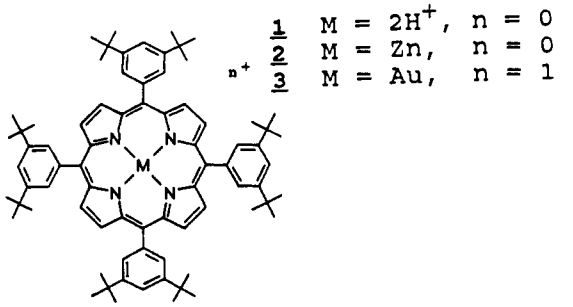

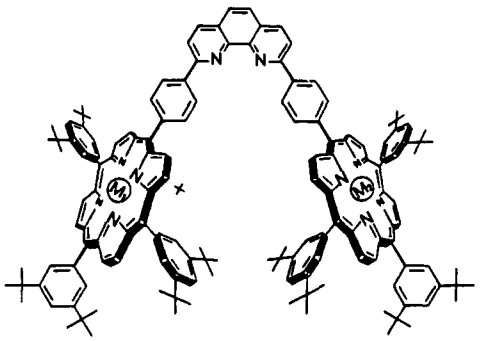

4 M_1 = Au; M_2 = Zn

5 M_1 = Au; M_2 = $2H^+$

Figure 1. Structures of the compounds studied in this work.

the natural photosynthetic light harvesting antennae.[6] Electron transfer has been observed, or implied, in many bisporphyrins.[1-4] Generally, these latter systems consist of a photoactive porphyrin component linked to a porphyrin subunit complexed to a high oxidation state metal which acts as an electron acceptor.[7] In contrast to the natural photosynthetic apparatus, these systems[7] store redox equivalents on one of the metal centers.

We describe here the photochemistry of oblique bisporphyrins comprising a gold(III) porphyrin and either a zinc(II) or a free-base porphyrin.[8] *The geometrical features of the bisporphyrins are well-defined and closely resemble those found in photosynthetic bacterial reaction center complexes.*[9,10] Rotation of the porphyrins about the spacer group is constrained,[11] although the geometry is not rigid, and the porphyrins are held at an average center-to-center separation of 13.6 Å. Previous work[7f] has shown that, for comparable zinc/iron(III) bisporphyrins, the rate of photoinduced charge separation depends weakly on separation distance but not on the apparent mutual orientation of the porphyrin rings. *It has been possible*, at least for the gold/zinc bisporphyrin, *to selectively excite each subunit in the bisporphyrin*, enabling a full photon balance to be made. Furthermore, the inherent photophysical properties of the individual porphyrins allow, for the first time, *formation of a common charge-transfer state from precursors of different spin multiplicity.*

Experimental Section

Porphyrins **1–5** were synthesized and purified as described elsewhere;[8] structures are given in Figure 1. Tetrakis(3,5-*tert*-butyl-4-hydroxyphenyl)porphyrin was available from a previous study.[12] All compounds gave satisfactory analyses and were further purified by TLC prior to making the photophysical measurements. *N,N*-Dimethylformamide (DMF) (Aldrich spectroscopic grade) was fractionally distilled from CaH_2. Absorption maxima (nm) (and molar extinction coefficients (M^{-1} cm^{-1})) for dilute DMF solutions are as follows: **1**, 412 (272 000), 518 (6740), 554 (4120), 592 (2490), 648 (2450); **2**, 429 (257 000), 562 (8700), 602 (5240); **3**, 416 (98 400), 526 (5140), 564 (740); **4**, 418 (239 000), 431 (257 000), 528 (12 300), 563 (11 700), 604 (7000); **5**, 418 (362 000), 520 (15 350), 552 (8540), 590 (2850), 648 (2340).

Absorption spectra were recorded with a Hewlett-Packard 8450A diode array spectrophotometer. Luminescence spectra were recorded with a Perkin-Elmer LS5 spectrofluorimeter and were corrected for wavelength responses of the detector.[13] Fluorescence quantum yields were measured relative to zinc tetraphenylporphyrin (ZnTPP) (Φ_f = 0.033).[14] Singlet excited state lifetimes were measured by time-correlated, single photon counting using a mode-locked Nd-YAG laser (Antares 76S) synchronously pumping a cavity-dumped Rhodamine 6G dye laser (Spectra Physics 375B/244). Glass cutoff filters were used to isolate fluorescence from scattered laser light. A Hamamatsu microchannel plate was used to detect emitted photons, for which the instrumental response function had an fwhm of 50 ± 10 ps. Data analyses were made according to O'Connor and Phillips[15] using computer deconvolution to minimize reduced χ^2 parameters. All solutions for fluorescence studies were optically dilute and air-equilibrated.

Flash photolysis studies were made with a frequency-doubled, Q-switched Quantel YG481 Nd-YAG laser (pulse width 10 ns, 200 mJ). The laser intensity was attenuated with crossed polarizers and calibrated using ZnTPP as the standard.[16,17] Solutions were adjusted to possess absorbances at 532 nm of ca. 0.2. Deoxygenation was achieved by N_2-purging. Differential absorption spectra were recorded point-by-point, with five individual laser shots being averaged at each wavelength. Kinetic measurements, averaging 50 individual laser shots, were made by computer nonlinear, least-squares iterative procedures.

Molar extinction coefficients for the triplet-state differential absorption spectra were determined by the complete conversion method.[18] A dilute, N_2-saturated DMF solution of the porphyrin was excited with a 10-ns laser pulse at 532 nm, and the absorbance change at the appropriate maximum was monitored. The laser intensity was increased from an initial value of 10 mJ until the transient absorbance change reached a plateau. Conditions were obtained for which all the porphyrin molecules within the laser optical pathway could be converted into metastable species, and the transient differential extinction coefficients were calculated from the initial porphyrin concentrations.

Improved time resolution was achieved with a frequency-doubled, mode-locked Quantel YG402 Nd-YAG laser (pulse width 30 ps).[19] For some studies, the excitation pulse was Raman shifted by focusing into a 10-cm path length cell containing perdeuterated cyclohexane. Glass filters were used to isolate the resultant 598-nm pulse. Laser intensities were attenuated in order to avoid two-photon absorption by a single bisporphyrin molecule, and 300 laser shots were averaged for each measurement. Solutions were adjusted to possess absorbances of ca. 0.4 at the excitation wavelength. Residual 1064-nm output from the laser was focused into 1/1 D_3PO_4/D_2O to produce a white light continuum for use as the analyzing beam. Variable delay times in the range 0–6

(5) (a) Anton, J. A.; Loach, P. A.; Govindjee *Photochem. Photobiol.* **1978**, *28*, 235. (b) Brookfield, R. L.; Ellul, H.; Harriman, A.; Porter, G. *J. Chem. Soc., Faraday Trans. 2* **1986**, *82*, 219. (c) Mialocq, J.-C.; Giannotti, C.; Maillard, P.; Momenteau, M. *Chem. Phys. Lett.* **1984**, *112*, 87. (d) Regev, A.; Galili, T.; Levanon, H.; Harriman, A. *Chem. Phys. Lett.* **1986**, *131*, 140. (e) Chardon-Noblat, S.; Sauvage, J.-P.; Mathis, P. *Angew. Chem., Int. Ed. Engl.* **1989**, *28*, 593. (f) Sessler, J. L.; Johnson, M. R.; Lin, T.-Y. *Tetrahedron* **1989**, *45*, 4767.

(6) Davila, J.; Harriman, A.; Milgrom, L. R. *Chem. Phys. Lett.* **1987**, *136*, 427.

(7) (a) Schwartz, F. P.; Gouterman, M.; Muljiani, Z.; Dolphin, D. *Bioinorg. Chem.* **1972**, *2*, 1. (b) Fujita, I.; Netzel, T. L.; Chang, C. K.; Wang, C.-B. *Proc. Natl. Acad. Sci. U.S.A.* **1982**, *79*, 413. (c) Brookfield, R. L.; Ellul, H.; Harriman, A. *J. Chem. Soc., Faraday Trans. 2* **1985**, *81*, 1837. (d) Heiler, D.; McLendon, G.; Rogalskyj, P. *J. Am. Chem. Soc.* **1987**, *109*, 604. (e) Mataga, N.; Yao, H.; Okada, T.; Kanda, Y.; Harriman, A. *Chem. Phys.* **1989**, *131*, 473. (f) Osuka, A.; Maruyama, K.; Mataga, N.; Asahi, T.; Yamazaki, I.; Tamai, N. *J. Am. Chem. Soc.* **1990**, *112*, 4958.

(8) Heitz, V.; Chardon-Noblat, S.; Sauvage, J.-P. *Tetrahedron Lett.* **1991**, *32*, 197. A related zinc(II)/free-base bisporphyrin has been described: see ref 5e.

(9) Deisenhofer, J.; Epp. O.; Miki, K.; Huber, R.; Michel, H. *J. Mol. Biol.* **1984**, *180*, 385.

(10) Chang, C.-H.; Tiede, D.; Tang, J.; Smith, U.; Norris, J. R.; Schiffer, M. *FEBS Lett.* **1986**, *205*, 82.

(11) Chardon-Noblat, S.; Guilhem, J.; Mathis, P.; Pascard, C.; Sauvage, J.-P. In *Photoconversion Processes for Energy and Chemicals*; Hall, D. O., Grassi, G., Eds.; Elsevier: London, 1989; p 90.

(12) Milgrom, L. R.; Mofidi, N.; Harriman, A. *J. Chem. Soc., Perkin Trans. 2* **1989**, 805.

(13) Argauer, R. J.; White, C. E. *Anal. Chem.* **1964**, *36*, 368.

(14) Egorova, G. D.; Knyukshto, V. N.; Solovev, K. N.; Tsvirko, M. P. *Opt. Spectrosc. (Engl. Transl.)* **1980**, *48*, 602.

(15) O'Connor, D. V.; Phillips, D. *Time Resolved Single Photon Counting*; Academic Press: London, 1984.

(16) Pekkarinen, L.; Linschitz, H. *J. Am. Chem. Soc.* **1960**, *82*, 2407.

(17) Hurley, J. K.; Sinai, N.; Linschitz, H. *Photochem. Photobiol.* **1983**, *38*, 9.

(18) Bensasson, R. V.; Land, E. J.; Truscott, T. G. *Flash Photolysis and Pulse Radiolysis: Contributions to the Chemistry of Biology and Medicine*; Pergamon Press: Oxford, 1983.

(19) Atherton, S. J.; Hubig, S. M.; Callen, T.; Duncanson, J. A.; Snowden, P. T.; Rodgers, M. A. J. *J. Phys. Chem.* **1987**, *91*, 3137.

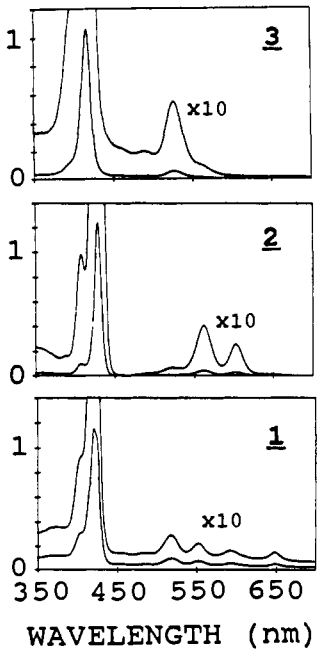

Figure 2. Absorption spectra recorded for the monomeric porphyrins in dilute DMF solution.

Table I. Properties of the Monomeric Porphyrins in DMF Solution

property	compound 1	2	3
E_s (eV)	1.90	2.06	2.21
Φ_f	0.19	0.045	<0.0001
τ_s (ns)	9.3	2.3	
E_t/eV	1.44	1.64	1.82
Φ_t	0.61	0.72	1.0
τ_t (μs)	1200	820	0.0014
$E_{red}°$ (V vs SCE)	−1.24	−1.63	−0.59
$E_{ox}°$ (V vs SCE)	1.01	0.62	1.62
$^sE_{red}°$ (V vs SCE)	0.66	0.43	1.62
$^tE_{red}°$ (V vs SCE)	0.20	0.01	1.23
$^sE_{ox}°$ (V vs SCE)	−0.89	−1.44	−0.59
$^tE_{ox}°$ (V vs SCE)	−0.43	−1.02	−0.20

ns were selected in a random sequence, and transient spectra were recorded with an Instruments SA UFS200 spectrograph interfaced to a Tracor Northern 6200 MCA and a microcomputer. Kinetic analyses were made by overlaying about 30 individual spectra and fitting data at selected wavelengths using computer nonlinear, least-squares iterative procedures. Error limits are given in the text.

Electrochemical measurements were made using differential pulse and cyclic voltammetry techniques. The porphyrins were dissolved in dried DMF containing tetra-*n*-butylammonium perchlorate (0.2 M) and were purged thoroughly with Ar. A Pt microelectrode was used as the working electrode, together with a Pt counter electrode, and an SCE reference. Redox potentials had a reproducibility of ±20 mV.

Results and Discussion

Properties of the Monomeric Porphyrins 1–3. Absorption and luminescence properties recorded for compounds **1–3** remain in good agreement with those reported for the corresponding tetraphenylporphyrins.[20] Absorption spectra for **1–3** in DMF are given in Figure 2 and exhibit the expected Sôret and Q-band transitions.[20] The spectra are characteristic of the cations residing in the porphyrin cavity;[20] quantitative data are provided in the Experimental Section. The lowest energy absorption transition was used to calculate the energy of the porphyrin first excited (π,π^*) singlet state (E_s), and the values are compiled in Table I. Both **1** and **2** fluoresce in DMF at room temperature, and the measured fluorescence quantum yields (Φ_f) and lifetimes (τ_s) (Table I) are comparable to values reported for related porphyrins.[21,22] As expected,[23] **3** is nonfluorescent due to the internal heavy-atom effect. Phosphorescence was observed from both **2** and **3** in methanol glasses at 77 K (Figure 3) and was used to derive the energy of the first excited (π,π^*) triplet state (E_t) (Table I). Since **1** is insoluble in alcohols, and DMF does not form an optical glass, the triplet energy of this compound was assumed to be identical to that of tetrakis(3,5-*tert*-butyl-4-hydroxyphenyl)porphyrin (**6**) in methanol (Figure 3) (Table I).

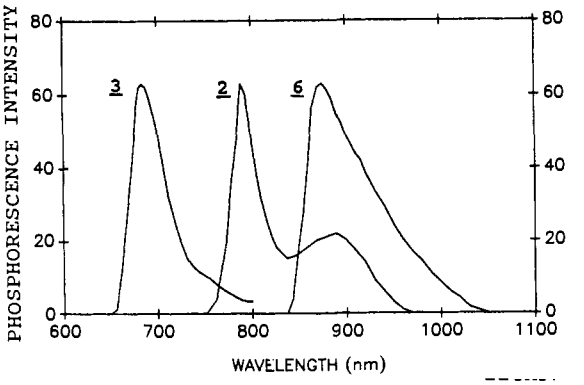

Figure 3. Phosphorescence spectra recorded in methanol glasses at 77 K for **2**, **3**, and tetrakis(3,5-*tert*-butyl-4-hydroxyphenyl)porphyrin (**6**).

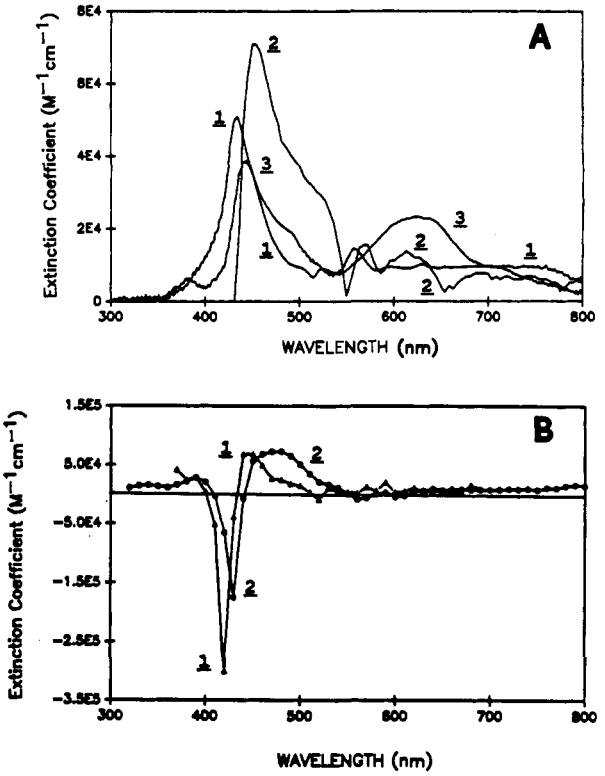

Figure 4. (A) Transient differential absorption spectra recorded immediately after excitation of the monomer porphyrins with a 30-ps laser pulse at 532 nm. (B) Transient differential absorption spectra recorded 1 μs after excitation of the monomer porphyrins with a 10-ns laser pulse at 532 nm.

Transient differential absorption spectra recorded after excitation of the porphyrins in DMF with a 30-ps laser pulse at 532 nm are shown in Figure 4a. For **1** and **2**, these spectra are assigned to the first excited singlet state by comparison to literature spectra.[24] These species decay on the nanosecond time scale to

(20) Gouterman, M. In *The Porphyrins*; Dolphin, D., Ed.; Academic Press: New York, 1978; Vol. 3, p 1.

(21) Harriman, A. *J. Chem. Soc., Faraday Trans. 1* **1980**, *76*, 1978.
(22) Harriman, A. *J. Chem. Soc., Faraday Trans. 2* **1981**, *77*, 1281.
(23) Antipas, A.; Dolphin, D.; Gouterman, M.; Johnson, E. C. *J. Am. Chem. Soc.* **1978**, *100*, 7705.
(24) Rodriguez, J.; Kirmaier, C.; Holten, D. *J. Am. Chem. Soc.* **1989**, *111*, 6500.

Table II. Reaction Exothermicities Calculated for the Various Photoinduced Electron-Transfer Processes Possible in the Bisporphyrins **4** and **5**

donor	acceptor	$\Delta G°$ (eV mol^{-1})
^{s}1	3	−0.30
^{t}1	3	+0.16
^{s}2	3	−0.85
^{t}2	3	−0.43
1	^{t}3	−0.22
2	^{t}3	−0.61
^{t}3	1	+1.04
^{t}3	2	+1.43
3	s_1	+0.96
3	t_1	+1.42
3	^{s}2	+1.19
3	^{t}2	+1.61

produce long-lived triplet excited states,[16,17] whose spectra are given in Figure 4b. The spectrum observed for **3** (Figure 4a) decays via first-order kinetics with a lifetime of 1.4 ± 0.2 ns to reform the ground state, and since this compound is nonfluorescent but phosphoresces strongly, it is assigned to the first excited triplet state. Quantum yields for formation of the triplet states (Φ_t) and triplet lifetimes (τ_t) recorded in deoxygenated DMF are given in Table I. Again, the values are in keeping with related porphyrins.[20-23]

In DMF **1**–**3** undergo a series of reversible oxidation and reduction steps. Redox potentials for one-electron reduction ($E_{red}°$) and oxidation ($E_{ox}°$) for each of the porphyrins are collected in Table I. The derived values remain similar to those reported for related porphyrins,[25] and the energy difference between addition and removal of one electron is 2.25 ± 0.05 eV, as expected for tetraphenylporphyrins.[25] This latter finding, taken together with earlier work,[26-29] is consistent with both reduction and oxidation processes involving only the tetrapyrrolic ring. Redox potentials for the respective excited states ($^{s/t}E_{red}°$ and $^{s/t}E_{ox}°$) are given also in Table I.[30]

Energy Gaps and Favorable Processes. It is instructive to use the data collected in Table I to predict the spontaneity of energy- and electron-transfer processes that could occur within the bisporphyrins **4** and **5**. Thus, the singlet and triplet electronic energy levels decrease in the order **3** > **2** > **1**, and solely on energetic grounds, triplet energy transfer could occur from the gold porphyrin subunit to either zinc (ΔE_{tt} = 0.18 eV) or free-base (ΔE_{tt} = 0.38 eV) porphyrins. Singlet energy transfer could occur also from gold porphyrin to zinc or free-base porphyrins, but the short lifetime of the donor makes this process unlikely.

The gold porphyrin subunit is expected to be reduced by the excited singlet states of **1** and **2** and by the excited triplet state of **2**; each respective reaction exothermicity ($\Delta G°$)[31] is provided in Table II. It is predicted also that the gold porphyrin excited triplet state could be reduced by either zinc or free-base porphyrins. In contrast, none of the reactions involving oxidation of the gold porphyrin subunit are expected to proceed spontaneously.

Conformation of the Bisporphyrins. The bisporphyrins possess two degrees of rotational freedom; each tetrapyrrolic ring can rotate about the C–C bond connecting it to the phenanthroline polycycle. An X-ray crystallographic study carried out with the biszinc complex showed[11] that two conformations exist in the solid state. One conformer corresponds to an endo, endo disposition: The water molecules attached to the zinc centers both point inward, giving rise to a porphyrin/porphyrin center-to-center separation of 13.8 Å and an interplanar angle of 87°. The second conformer has an endo, exo arrangement: One water molecule is turned toward the center of the bisporphyrin whereas the other points to the outside, giving a center-to-center separation of 13.4 Å and an interplanar angle of 67°.

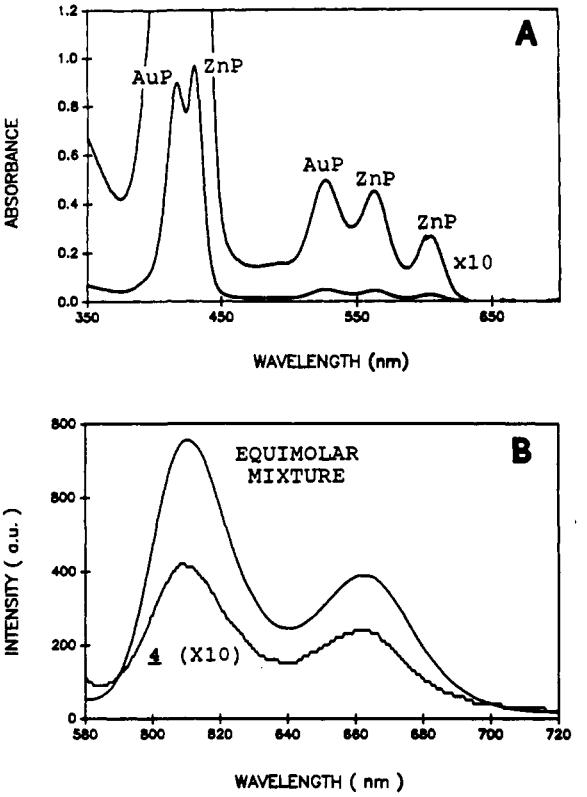

Figure 5. (A) Absorption spectrum recorded for **4** in dilute DMF solution. The individual bands are assigned to zinc (ZnP) or gold (AuP) porphyrin subunits according to the spectra recorded for the monomeric porphyrins **2** and **3**. (B) Fluorescence spectra recorded for **4** and an equimolar mixture of **2** + **3**.

Gold(III) and free-base porphyrins do not possess axial ligands, and consequently, the gold(III) porphyrin is monocationic. Our studies were made with the PF_6^- salt, and it was observed that addition of excess NH_4PF_6 did not affect the photophysical properties of **4**. Similarly, NH_4PF_6 does not quench the excited singlet or triplet states of **1** or **2** in DMF or methanol solutions.

Photochemistry of the Gold/Zinc Bisporphyrin 4. The absorption spectrum of the bisporphyrin **4** in DMF is a superimposition of spectra of **2** and **3**, indicating that there is little electronic coupling between the linked porphyrins. As shown by Figure 5a, the two Sôret bands are distinct and can be assigned to the individual gold(III) and zinc(II) porphyrin subunits whereas the Q-band region indicates three transitions. The two lowest energy absorption bands are associated with the zinc(II) porphyrin subunit whereas the higher energy band is characteristic of the gold(III) porphyrin. In DMF at room temperature weak fluorescence is observed which bears the characteristics of emission from a zinc porphyrin (Figure 5b). The excitation spectrum closely resembles the excitation and absorption spectra recorded for **2**, indicating that singlet energy transfer from gold(III) to zinc(II) porphyrins does not occur. Presumably, this is because of the very short lifetime of the donor. Excitation of **4** at a wavelength where only the zinc(II) porphyrin subunit absorbs gave a fluorescence quantum yield of 0.0012 ± 0.0002[32] and a fluorescence lifetime

(25) (a) Felton, R. H. In *The Porphyrins*; Dolphin, D., Ed.; Academic Press: New York, 1978; Vol. 5, p 53. (b) Harriman, A.; Richoux, M.-C.; Neta, P. *J. Phys. Chem.* **1983**, *87*, 4957.
(26) Fleischer, E. B.; Laszio, A. *Inorg. Nucl. Chem. Lett.* **1969**, *5*, 373.
(27) Jamin, M. E.; Iwamoto, R. T. *Inorg. Chim. Acta* **1978**, *27*, 136.
(28) Carnieri, N.; Harriman, A. *Inorg. Chim. Acta* **1982**, *62*, 103.
(29) Segawa, H.; Nishino, H.; Kamakawa, T.; Honda, K.; Shimidzu, T. *Chem. Lett.* **1989**, 1917.
(30) Calculated according to $^{ox}E_{ox}° = E_{ox}° - E_{es}$ and $^{ox}E_{red}° = E_{red}° + E_{es}$, where E_{es} is the excitation energy of the excited singlet or triplet state.
(31) Calculated according to $\Delta G_{ct}° = E_{red}° - E_{ox}° - E_{es}$, where $E_{ox}°$ and $E_{red}°$ refer to the one-electron redox potentials for oxidation and reduction of the individual porphyrin subunits, respectively, and E_{es} in the excitation energy of the porphyrin excited singlet or triplet state as determined from luminescence or absorption spectroscopy.
(32) An identical value was obtained by comparing the fluorescence yield for **4** with that from a 1/1 molar mixture of **2** + **3** and exciting at different wavelengths.

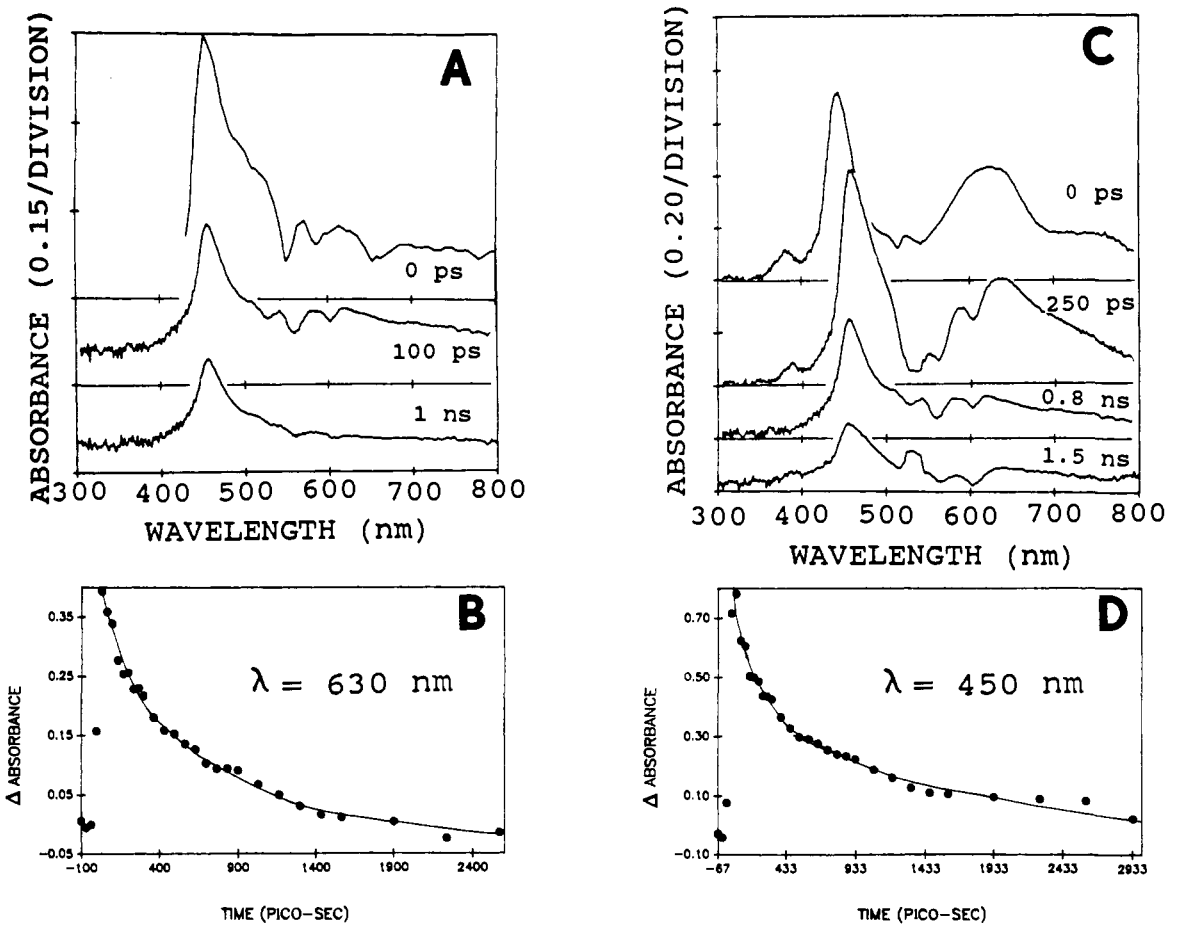

Figure 6. (A) Transient absorption spectra recorded after excitation of **4** in DMF with a 30-ps laser pulse at 598 nm; delay times are given on the traces. (B) Typical kinetic trace observed for the conditions as in (A). (C) Transient absorption spectra recorded after excitation of **4** in DMF with a 30-ps laser pulse at 532 nm. (D) Typical kinetic trace observed for the conditions as in (C).

of 55 ± 5 ps. Comparison with **2** shows that fluorescence from the zinc(II) porphyrin subunit is quenched by ~97%.

Excitation of **4** with a 30-ps laser pulse at 598 nm, where only the zinc porphyrin subunit absorbs, forms the excited singlet state of the zinc porphyrin (Figure 6a). This species can be identified by comparison of its absorption spectrum with that characterized[24] for **2** under identical conditions (Figure 4a). The excited singlet state decays rapidly to form a transient exhibiting pronounced absorption at 440 nm and between 640 and 750 nm and which decays with a lifetime of 600 ± 40 ps (Figure 6b). This transient can be assigned to a charge-transfer (CT) state in which an electron has been transferred from the excited singlet state of the zinc porphyrin to the adjacent gold porphyrin.[33] This process, which results in formation of the zinc porphyrin π-radical cation and the neutral gold(III) porphyrin radical, is better described as a "charge shift reaction" than as a conventional "charge separation process". Decay of the CT state ($^{+\cdot}$ZnP–AuP$^{\cdot}$) regenerates the ground-state bisporphyrin without involving any other spectroscopically detected species. Thus, excitation of the zinc porphyrin subunit in **4** leads to rapid charge transfer followed by slower reverse electron transfer (Figure 7). The rate constants and reaction exothermicities for the various steps are compiled in Table III.

$$\text{ZnP–AuP}^{+} \underset{}{\overset{h\nu}{\rightleftharpoons}} {}^{+\cdot}\text{ZnP–AuP}^{\cdot} \qquad (1)$$

(33) Absorption spectra of closely related zinc(II) porphyrin π-radical cations (Carnieri, N.; Harriman, A. *Inorg. Chim. Acta* **1982**, *62*, 103) and one-electron-reduced gold(III) porphyrins (Abou-Gamra, Z.; Harriman, A.; Neta, P. *J. Chem. Soc., Faraday Trans. 2* **1986**, *82*, 2337) have been described. Reference 29 describes the formation of a ground-state complex between zinc and gold porphyrins in aqueous solution which undergoes photoinduced charge transfer.

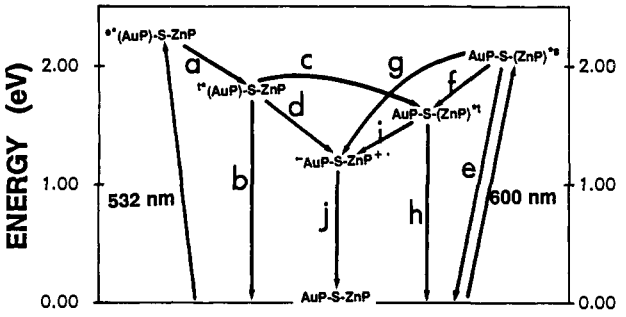

Figure 7. Overall reaction scheme for photoinduced electron transfer in the zinc/gold bisporphyrin **4**. Rate constants (s^{-1}) and quantum efficiencies for the various processes are as follows: (a) $>10^{12}$, 100%; (b) 7×10^{8}, 8%; (c) 1.2×10^{9}, 15%; (d) 6.4×10^{9}, 77%; (e) 4×10^{7}, ~0.2%; (f) 4×10^{8}, 2%; (g) 1.8×10^{10}, 98%; (h) 1.2×10^{3}; (i) 7.7×10^{8}, 100%; (j) 1.7×10^{9}.

Table III. Effect of Reaction Exothermicity on the Rate Constants for Charge Transfer and Reverse Electron Transfer in the Bisporphyrins **4** and **5**

donor	acceptor	$\Delta G_{ct}°$ (eV)	log k_{ct}	$\Delta G_{ret}°$ (eV)	log k_{ret}
ZnP	^{t}AuP	−0.61	9.81	−1.21	9.24
^{s}ZnP	AuP	−0.85	10.25	−1.21	9.22
^{t}ZnP	AuP	−0.43	8.89	−1.21	
H_2P	^{t}AuP	−0.22	8.79	−1.60	
$^{s}H_2P$	AuP	−0.30	8.62	−1.60	
$^{t}H_2P$	AuP	+0.16	3.43	−1.60	

Immediately after excitation of **4** with a 30-ps laser pulse at 532 nm, where the gold porphyrin subunit absorbs ca. 85% of incident photons,[34] the gold porphyrin excited triplet state can be

observed (Figure 6c). This species decays with a lifetime of 120 ± 10 ps, compared to a value of 1.4 ± 0.1 ns measured for **3**, to form a mixture of two products. The shorter lived product, which accounts for 77% of the decay of the gold porphyrin excited triplet state,[35] corresponds to the CT state, as described for excitation at 598 nm. This species decays with a lifetime of 570 ± 30 ps due to reverse electron transfer (Figure 6d). The longer lived product is the triplet excited state of the zinc porphyrin subunit (Figure 6c), as characterized by its absorption spectrum[16,17] which is similar to that of **2**. Because of its relatively high yield,[35] it appears that this species arises from energy transfer from the gold porphyrin triplet. On the basis of extinction coefficients measured for the triplet states of **2** and **3**, the yield of the triplet energy transfer process is ca. 15% and, therefore, the rate constant is ca. 1.2×10^9 s^{-1}.[35]

The excited triplet state of the zinc porphyrin subunit within **4** decays with a lifetime of 1.3 ± 0.2 ns. This is much shorter than that measured for **2**, where τ_t is 820 ± 50 μs in deoxygenated DMF. It seems probable that triplet quenching involves intramolecular electron transfer to the appended gold(III) porphyrin (Figure 7). The rate constant for this step ($k = (7.7 \pm 1.2) \times 10^8$ s^{-1}) indicates that charge transfer should be quantitative. Because the CT state survives for only ~600 ps, reverse electron transfer occurs within the zinc porphyrin triplet lifetime and the CT state was not detected in the flash photolysis records.

Excitation of either porphyrin subunit in **4** results in electron transfer from zinc to gold porphyrins to form the CT state (Figure 7). For the zinc porphyrin, both singlet and triplet excited states function as electron donors whereas for the gold porphyrin intersystem crossing to the triplet manifold is quantitative and the triplet acts as an electron acceptor. *Consequently, virtually every photon absorbed by the bisporphyrin results in charge transfer* (Figure 7).

Photochemistry of the Free-Base/Gold Bisporphyrin 5. The absorption spectrum of **5** in DMF corresponds to a superimposition of spectra of the individual porphyrins, but the Sôret region appears as a single band and the Q-band of the gold porphyrin subunit cannot be resolved clearly. Weak fluorescence ($\Phi_f = 0.037 \pm 0.004$) is observed on excitation into the free-base porphyrin absorption bands (520 or 590 nm) for which the lifetime was measured to be 1.9 ± 0.2 ns. Comparison with **1** indicates that the degree of fluorescence quenching in **5** is ca. 80%.

Excitation of **5** with a 30-ps laser pulse at 598 nm, where only the free-base porphyrin subunit absorbs, gives a transient absorption spectrum readily identified as that of the free-base excited singlet state.[24] It decays with a lifetime of 2.0 ± 0.3 ns to produce the triplet state of the free-base porphyrin[16,24] which, in turn, decays with a lifetime (τ_t) of 770 ± 50 μs in the absence of oxygen. From the picosecond flash photolysis records, the average absorbance ratio of singlet to triplet states at 440 nm, extrapolated to the center of the exciting laser pulse, was 5.86 ± 0.35 which, using the molar extinction coefficients measured for the corresponding monomer **1** (Figure 4), shows that the quantum yield for formation of the triplet state is 0.13 ± 0.008. This value is much lower than that measured for **1** ($\Phi_t = 0.61$) and indicates that an additional nonradiative process competes effectively with intersystem crossing. Presumably, this process involves electron transfer to the appended gold(III) porphyrin subunit, although the intermediate CT state was not observed in the picosecond laser flash photolysis records. This is consistent with the CT state having a lifetime similar to that found for the gold/zinc bisporphyrin. The derived rate constants and reaction exothermicities are compiled in Table III.

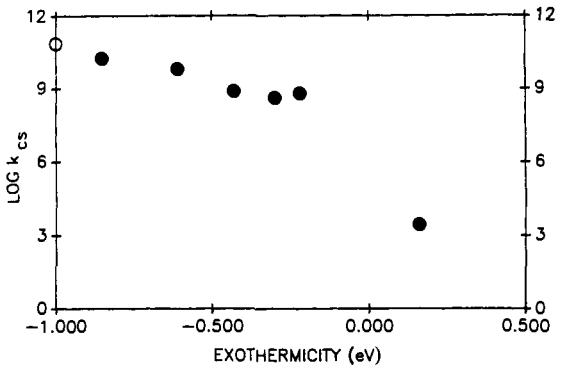

Figure 8. Correlation between rate constant for charge transfer (k_{ct}) and reaction exothermicity for the bisporphyrins **4** and **5**. The additional data point (○) is interpolated from ref 7f for a center-to-center separation distance of 13.6 Å.

$$H_2P\text{-}AuP^+ \overset{h\nu}{\rightleftharpoons} {}^{+\cdot}H_2P\text{-}AuP^{\cdot} \quad (2)$$

For the corresponding triplet-state reaction the quenching rate constant is only 2.7×10^3 s^{-1} (Table III) and no intermediate states were apparent in the flash photolysis records. In view of the very low rate constant, other quenching processes, such as long-range spin–orbital coupling, cannot be excluded.

Excitation of **5** with a 30-ps laser pulse at 532 nm, where the gold porphyrin absorbs ~40% of incident photons,[36] gives a mixture of gold porphyrin triplet and free-base singlet excited states. The free-base singlet state decays as described above ($\tau = 2.2 \pm 0.5$ ns). The gold porphyrin triplet excited state decays rapidly with a lifetime of 120 ± 20 ps. Comparison with **3** indicates that the rate constant for quenching the gold porphyrin triplet excited state is $(7.6 \pm 0.5) \times 10^9$ s^{-1}. This quenching process is expected to involve both triplet energy transfer and electron transfer.

The partition coefficient and ensuing rate constants were derived as follows: The yield of the free-base porphyrin triplet excited state was measured after excitation of optically matched dilute DMF solutions of **5** and an equimolar mixture of **1** + **3** with a 10-ns laser pulse at 532 nm of varying intensity. The averaged absorbance ratio at 745 nm (where $\epsilon_t = 5300$ M^{-1} cm^{-1}) was 1.22 ± 0.06 for **5** relative to the equimolar mixture. Accepting that, for both samples, the free-base porphyrin subunit absorbs 60% of incident photons and using the above Φ_t values, we conclude that the fraction of the quenching process that results in triplet energy transfer within **5** is 92% ± 6%. This means that partition in favor of charge transfer from the gold porphyrin triplet state is only 8% ± 6%. The relevant rate constants then become 7.0×10^9 and 6.0×10^8 s^{-1}, respectively, for triplet energy transfer and electron transfer. However, we could not detect the CT state in the flash photolysis records, presumably because of its low yield. The increased partitioning in favor of triplet energy transfer is a consequence of the increased triplet energy gap and decreased exothermicity for electron transfer for **5** relative to **4**.

Correlation of Reaction Rates. The derived rate constants for intramolecular charge transfer (k_{ct}) and subsequent reverse electron transfer (k_{ret}) are compiled in Table III, together with the calculated reaction exothermicities. It is seen that k_{ct} increases smoothly with increasing exothermicity, throughout the range studied, reaching an apparent maximum around −1 eV where the

(34) This value was obtained by subtraction of the corrected excitation spectrum from the ground-state absorption spectrum, assuming no singlet energy transfer from gold to zinc porphyrins.

(35) This value is derived as follows: The differential absorbance at 630 nm observed immediately after the pulse is attributed solely to the triplet state of the gold porphyrin subunit whereas that remaining 2 ns after the pulse is attributed solely to the triplet state of the zinc porphyrin subunit. The maximum concentrations of the two triplets were calculated by computer extrapolation of the observed first-order decay profiles to the center of the exciting laser pulse using the molar extinction coefficients derived for the monomer porphyrins **2** ($\epsilon_t = 4000$ M^{-1} cm^{-1}) and **3** ($\epsilon_t = 23\,000$ M^{-1} cm^{-1}). In this manner, it was concluded that triplet energy transfer accounted for 15% ± 3% of the initially formed gold porphyrin triplet state. Since the inherent nonradiative deactivation accounts for 8% ± 2% of the triplet state, formation of the charge-transfer state must be responsible for the residual 77% ± 5%.

(36) This value was obtained by subtraction of the corrected excitation spectrum from the ground-state absorption spectrum, assuming no singlet energy transfer from gold to free-base porphyrins. A similar value was obtained by treating the bisporphyrin with trifluoroacetic acid which forms the dication of the free-base porphyrin but leaves the gold porphyrin unaffected. The porphyrin dication does not absorb in this region.

rate is $\sim 5 \times 10^{10}$ s^{-1} (Figure 8). This indicates that the reaction falls well within the "normal" region. The plot also includes a data point interpolated from the study by Osuka et al.[7f] involving charge transfer across an aryl-bridged zinc/iron(III) bisporphyrin at a center-to-center separation of 13.6 Å. Although this latter system involves reduction of the central iron(III) ion, rather than the porphyrin ring, k_{ct} correlates well with our data, suggesting similar reorganization energies for the two systems. The structure is such that electron transfer in the aryl-bridged bisporphyrin[7f] should proceed through the spacer, and consequently, it is likely that charge transfer in **4** and **5** also proceeds via a "through-bond" mechanism.

Our results give no information regarding the mechanism of triplet energy transfer although, in view of the relatively large distance, a Dexter mechanism seems appropriate.[37] It is interesting to note the large difference in rates of triplet energy transfer observed for **4** and **5** ($k_{tt}^5/k_{tt}^4 \approx 10$) in view of the almost constant k_{ct} ($k_{ct}^4/k_{ct}^5 \approx 1.3$)[38] over comparable energy gaps. Clearly, the two processes involve quite disparate energy gap dependences, and this finding will be explored further with more appropriate models.

The plateau region in Figure 8 is broad, and k_{ct} remains fairly insensitive to changes in reaction exothermicity over a wide energy range. This behavior, which has been observed for charge-shift reactions involving bimolecular species in frozen media[39] and in model calculations,[40] precludes meaningful determination of the coupling energy between the two porphyrin rings with the present data set. Osuka et al.[7f] found that the rate of reverse electron transfer ($k_{ret} \approx 5 \times 10^8$ s^{-1}) was independent of separation distance and mutual orientation for a range of covalently linked zinc/iron(III) bisporphyrins. For **4**, k_{ret} is 1.7×10^9 s^{-1}, which is a factor of 3 higher than for the zinc/iron(III) bisporphyrin although $\Delta G°$ is ca. −1.2 eV for both systems. The higher rate may be associated with reduction involving the porphyrin ring rather than the metal center.[41] *Furthermore, the same k_{ret} is observed for 4 regardless of the spin multiplicity of the precursor excited state.* This finding is consistent with the high spin–orbital coupling constant of the central gold(III) ion[23] which can affect the apparent spin of the CT state. This being the case, the lifetime of the CT state may be longer than that of a comparable bisporphyrin not possessing a heavy atom.

Acknowledgment. Support for this work was provided by the CNRS and by the Texas Advanced Research Program. The CFKR is supported jointly by the Division of Research Resources of the NIH (Grant RR00886) and by the University of Texas at Austin.

Registry No. 1, 89372-90-7; **2**, 116123-17-2; **3**, 136316-46-6; **4**, 133724-11-5; **5**, 133724-13-7.

(37) Closs, G. L.; Piotrowiak, P.; MacInnis, J. M.; Fleming, G. R. *J. Am. Chem. Soc.* **1988**, *110*, 2653.

(38) For comparison, k_{ct} values for the following couples were used: k_{ct}^4 refers to **4** with the zinc porphyrin triplet as donor and the gold porphyrin as acceptor and k_{ct}^5 refers to **5** with the gold porphyrin triplet as acceptor and the free-base porphyrin as donor.

(39) Miller, J. R.; Beitz, J. V.; Huddleston, R. K. *J. Am. Chem. Soc.* **1984**, *106*, 5057.

(40) Kakitani, T.; Mataga, N. *J. Phys. Chem.* **1987**, *91*, 6277.

(41) Osuka et al.[7f] comment that the ligand bound to the central iron(III) ion may play an important role in determining the magnitude of k_{ret} but not k_{ct}.

Enhanced Nickel(II) Chelation by *gem*-Dimethyl-Substituted Macrocyclic Tetrathioethers[1]

John M. Desper,[†] Samuel H. Gellman,*[,†] Robert E. Wolf, Jr.,[‡] and Stephen R. Cooper*[,‡]

Contribution from the S. M. McElvain Laboratory of Organic Chemistry, Department of Chemistry, University of Wisconsin, 1101 University Avenue, Madison, Wisconsin 53706, and Inorganic Chemistry Laboratory, University of Oxford, Oxford OX1 3QR, United Kingdom.
Received February 4, 1991

Abstract: The conformational and Ni(II)-binding properties of 1,4,8,11-tetrathiocyclotetradecane (**1**) and derivatives bearing *gem*-dimethyl pairs at the 6- or at the 6- and 13-positions (**2** and **3**, respectively) are compared. The syntheses and crystal structures of **2**, **3**, and their $Ni(ClO_4)_2$ complexes are reported; analogous data for **1** and its $Ni(BF_4)_2$ complex have been in the literature for some time. All three Ni(II) complexes show very similar 14-membered ring conformations, but the metal-free macrocycles display different conformations, in the solid state. These structural data suggest that each *gem*-dimethyl pair progressively biases the macrocycle toward the chelating conformation. We have examined the relative Ni(II) affinities of **1**–**3** in CD_3NO_2 by means of competition experiments monitored by ^1H NMR. Tetrathioether **2** binds Ni(II) approximately 7.3 times more tightly than does **1** at room temperature, and **3** binds Ni(II) approximately 49 times more tightly than does **1**. Thus, each *gem*-dimethyl pair leads to a 1.1 kcal/mol improvement in Ni(II) binding free energy under these conditions. We suggest that the incremental improvement in binding strength across the series **1**–**3** is correlated to the incremental changes in macrocycle conformation observed in the crystal structures of the metal-free thioethers.

Introduction

Ligands that can selectively bind late transition-metal ions are of practical interest because of the ecological and economic significance of these ions. Thioether sulfur is an appealing building block in this regard since it displays a selective affinity for late transition-metal ions relative to other cations.[2] Compared with the vast exploration of the impact of variations in polyether structure on oxophilic cation-binding properties,[3,4] however, relatively little effort has been devoted to examining the effect

[†] University of Wisconsin.
[‡] University of Oxford.

(1) This research was initiated independently in our two laboratories; for preliminary reports, see: (a) Wolf, R. E.; Cooper, S. R. Abstract INOR 173, 185th National Meeting of the American Chemical Society, Seattle, WA, 1983. (b) Desper, J. M.; Gellman, S. H. *J. Am. Chem. Soc.* **1990**, *112*, 6732.

(2) For leading references, see: (a) Cooper, S. R. *Acc. Chem. Res.* **1988**, *21*, 141. (b) Cooper, S. R.; Rawle, S. C. *Structure and Bonding* **1990**, *72*, 1.

(3) Pedersen, C. J. *J. Am. Chem. Soc.* **1967**, *89*, 2495.

0002-7863/91/1513-8663$02.50/0